RFP-2647
February 14, 1978

RFP-2647
February 14, 1978

INTERACTION OF XENON LIGHT WITH THE SURFACE OF 304 STAINLESS STEEL

Robert W. Krenzer

Research and Development
GENERAL METALLURGY GROUP

Rockwell International

Atomics International Division
Rocky Flats Plant
P.O. Box 464
Golden, Colorado 80401

U. S. DEPARTMENT OF ENERGY
CONTRACT EY-76-C-04-3533

DISCLAIMER

Printed in the United States of America
Available from the
National Technical Information Service
U. S. Department of Commerce
Springfield, Virginia 22161
Price: Printed Copy $4.00 Microfiche $3.00
Price Is Subject to Change Without Notice

Printed
February 14, 1978

RFP-2647
UC-25 MATERIALS
TID-4500-R66

INTERACTION OF XENON LIGHT WITH THE SURFACE OF 304 STAINLESS STEEL

Robert W. Krenzer

Research and Development,
GENERAL METALLURGY GROUP

SUBJECT DESCRIPTORS

304 Stainless Steel
Laser Amplifiers
Xenon Light
Thermal Etching

ROCKWELL INTERNATIONAL
ATOMICS INTERNATIONAL DIVISION
ROCKY FLATS PLANT
P. O. BOX 464
GOLDEN, COLORADO 80401

Prepared under Contract EY-76-C-04-3533
for the
Albuquerque Operations Office
U. S. Department of Energy

CONTENTS

ACKNOWLEDGEMENTS

The author would like to acknowledge V. K. Grotzky and J. F. Capes for their able assistance with the scanning-electron microscope work, and A. W. Brewer and the Metallurgical Laboratory for their metallographic support.

INTERACTION OF XENON LIGHT WITH THE SURFACE OF 304 STAINLESS STEEL

Robert W. Krenzer

Abstract. Laser amplifier frames fabricated from Type 304 stainless steel are known to cause damage to glass lenses by ejecting particles which are deposited on the lenses. High energy pulses of xenon light interact with the steel surface to produce damage sites. Heat treatment and surface cleaning procedures greatly affect the surface stability of the steel and influence contamination generated by the steel. It is believed that inclusions and/or carbides play a role, and the size of damage sites observed on glass correlate with the size of nonmetallic phases in the steel. Thermal etching of the steel was found to be a principle mechanism of surface damage caused by the high energy xenon light.

INTRODUCTION

Austenitic stainless steels, such as Type 304, are known for excellent corrosion resistance. However, such steels are susceptible to intergranular attack in certain environments (1).[1] Several theories have been proposed to explain this localized attack at grain boundaries, and derived mechanisms to explain observed corrosion behavior have been based on a chromium depletion theory (2, 3), solute segregation theory (4, 5), strain energy theory (6, 7), and electrochemical theory (8, 9, 10). Although differences of opinion exist as to the exact nature of the corrosion attack, it is generally recognized that the weakest link in the ability of stainless steel to resist corrosion is the grain boundaries. The chemistry and microstructure of the grain boundaries in the steel have a direct bearing on its corrosion susceptibility.

The microstructure of grain boundaries in Type 304 can be drastically changed by heat treatment. Type 304 stainless steel is solution treated in the temperature range of 1000 to 1125 °C to insure maximum corrosion resistance. During solution treatment, carbides which form in grain boundaries are dissolved. Between 450 and 900 °C, carbide precipitation occurs. The morphology of the carbides can be classified into three distinct types (11). At the highest temperatures, around 800 to 900 °C, a discontinuous network of separate particles is formed and the alloy is referred to as being stabilized. At intermediate temperatures, between 700 and 800 °C, carbide dentrites form in the boundaries. Between 450 and 700 °C, a continuous film of carbides precipitate in the boundaries and the alloy in this condition is referred to as being sensitized. These microstructural changes in the size and distribution of carbides in the grain boundaries can produce variable effects in the corrosion behavior of the steel.

In the present work, it is of interest to identify the source of particle contamination in laser amplifiers. During the operation of the laser, small particles are deposited on the elliptical lenses inside the amplifiers. Such damage sites on the lenses produce a nonuniform laser beam. The main frame of the amplifier is fabricated from Type 304 stainless steel. Although the laser beam does not directly contact the steel, high energy pulses of xenon light interact with the steel surface. It has been suggested that particles either loosely attached to the metal surface and/or within a thin layer next to the surface can be ejected by the high energy pulses and create a damage site on the lenses. The purpose of this study is to identify the damage mechanism and determine how to eliminate the problem.

The approach taken in this study is to assume that xenon light can damage the steel surface in a

[1] Numerals in parentheses relate to references at end of text.

similar manner to known corrosion behavior, and that localized attack of inclusions in the steel can produce the observed damage sites. The effect of high energy pulses of xenon light in a partial pressure of nitrogen on the surface of stainless steel is unknown. To obtain clean metal surfaces, amplifier frames are electropolished, chemical polished, and buffed. This initial phase of the study is designed to look at the effect of heat treatment and surface polishing on the surface condition of the steel and to determine if carbide precipitation plays a role as a source of damage sites.

EXPERIMENTAL PROCEDURE

Samples for this study were prepared from Type 304 stainless steel sheet having the chemistry listed in Table I. The surface condition of the as-received sheet is typical of rolled product, with numerous scratches and a fairly rough, irregular surface. Samples, 3.49 by 1.27 by 0.16 cm., were sheared out of the sheet. Except for grinding the edges of the samples to remove the sharp edges after shearing, no machining was performed on the sample surfaces. Thus, the starting surface condition was typical of rolled product with no specified heat-treated condition.

Various heat treatments and surface cleaning treatments were examined. Sample identification, together with a description of the heat treatments and surface treatments used, are tabulated in Table II. Except for as-received samples, all were first solution treated at 1050°C in vacuum prior to subsequent heat treatments and surface treatments. After solution treatment, samples were quenched in helium to cool below 400°C within three minutes. Three samples were then prepared from each set of heat treatments and surface treatments.

To simulate conditions existing in the laser amplifiers, samples were flashed at Lawrence Livermore Laboratory (LLL) in a helical flashlamp chamber. The standard test used to evaluate the cleanliness of a metal in the amplifier environment is to encapsulate a sample in quartz containing a partial nitrogen pressure of about 0.8 atmospheres, then flash the sample 50 times with xenon light.

TABLE I. Chemical Composition of Type 304 Stainless Steel

Element	Weight Percent
Carbon (C)	0.070
Chromium (Cr)	19.59
Nickel (Ni)	10.68
Manganese (Mn)	1.47
Molybdenum (Mo)	0.25
Silicon (Si)	0.62
Sulfur (S)	0.024
Oxygen (O_2)	0.014
Aluminum (Al)	< 0.001
Titanium (Ti)	< 0.001
Phosphorus (P)	0.05

TABLE II. Heat Treatment and Polishing Procedures

I. Heat Treatments
   - A. Solution treatment - 1050 °C for 1 hr., WQ
   - B. Stabilization - 850 °C for 2 hrs., AC
   - C. Sensitization - 650 °C for 2 hrs., AC

II. Surface Treatments
   - A. Electropolish - electroglow solution (H_3PO_4 + H_2SO_4) 50 °C, 8 volts for 4 minutes, rinsed in distilled H_2O and alcohol
   - B. Chemical polish - 95% H_3PO_4, 5% HF 50 °C, submerge for 10 minutes, rinsed in distilled H_2O

Damage sites resulting from this interaction of the pulsed energy with the metal surface can be observed on the interior surface of the quartz capsule, and a quantitative rating system, based on the number of damage sites, established from previous experience of flashing specimens, was used to rate the surface cleanliness of a sample (12). A sample which would produce very few or no damage sites under these conditions would be representative of a clean metal with a stable surface, and would be a desirable material for fabricating amplifier frames. Samples in the various conditions were examined, both optically and with the scanning-electron microscope (SEM), before and after

flashing. Damage sites on the quartz were also examined with the SEM to identify the chemical composition of the sites.

RESULTS

Metallography

The Type 304 steel sheet used in this study was typical of commercial purity, fully annealed sheet. The sheet contained numerous inclusions, as shown in Figure 1, aligned in stringers parallel to the rolling direction. The majority of the inclusions varied from approximately 5 to 25 microns in width, and up to about 50 microns maximum length. The grain structure near the surface of the as-received sheet is slightly duplexed, with a grain size ranging from ASTM 6 to 9.

It should be noted that there is a difference between inclusions and carbides referred to in this study. The term inclusions refers to nonmetallic phases (oxides, sulfides, and silicates) that are present within the grains. Carbides refer to the phases that precipitate in the grain boundaries. The different heat treatments used in this study are intended to affect the size and distribution of carbides in the boundaries, and will have very little, if any, effect on the inclusions in the matrix. The inclusion content can be reduced by improving the melting practice and increasing the purity of the steel. Carbides in the grain boundaries can be eliminated by solution treatment.

All of the samples were initially solution-treated at 1050°C for one hour. Some samples were subsequently heat treated at lower temperatures to either sensitize or stabilize the alloy. All three heat treated conditions resulted in fairly equivalent grain structures, heavily duplexed with a grain size ranging from ASTM 1 to 7, as typified in the stabilized sample shown in Figure 2.

FIGURE 1. Microstructure of As-Received Type 304 Stainless Steel. Magnification 100X.

FIGURE 2. Microstructure of Sample Solution Treated at 1050 °C, then Stabilized at 850 °C. Magnification 100X.

(a)

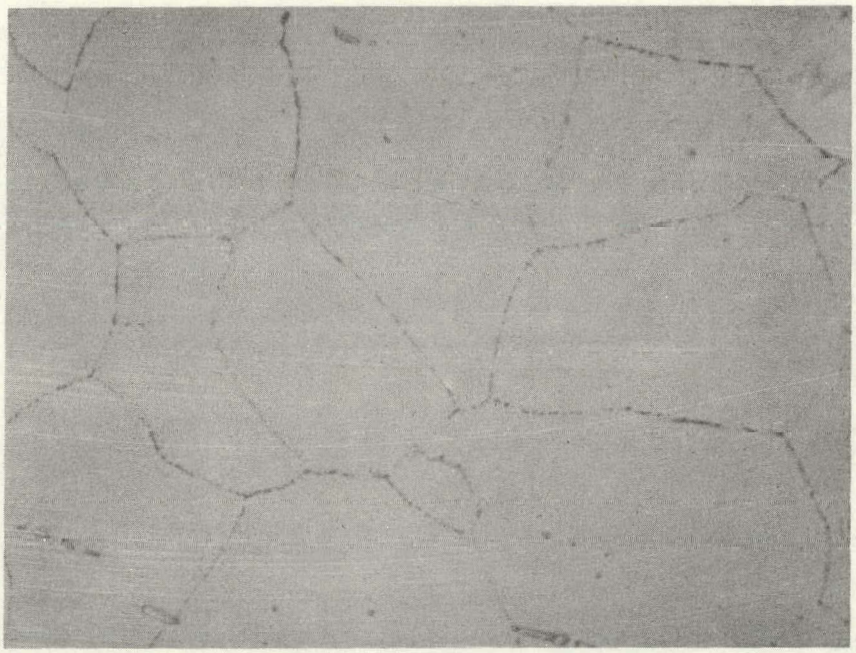

(b)

FIGURE 3. Grain Boundary Carbide Precipitation in the (a) Stabilized and (b) Sensitized Samples. Magnification 1200X.

TABLE III. Physical Appearance of Preflashed Samples

Heat Treatment	Surface Treatment	Surface Appearance	Grain Boundary Condition
Solution-Treated	Electropolished	Shiny, Smooth	Smooth
	Chemical Polished	Dull luster	Grain boundary attack
	Electropolished + Chemical Polished	Shiny, Smooth	Smooth
Stabilized	Electropolished	Heavily pitted	Heavy attack, large particles in boundaries
	Chemical Polished	Dull luster	Grain boundary attack
	Electropolished + Chemically Polished	Heavily pitted	Heavy attack, large particles in boundaries
Sensitized	Electropolished	Slight pitting	Moderate attack, continuous grain boundary film
	Chemical Polished	Dull luster	Grain boundary attack
	Electropolished + Chemical Polished	Moderate pitting	Moderate attack, continuous grain boundary film

At high magnifications, microstructural differences between samples solution-treated, and either sensitized or stabilized, were readily apparent. The grain boundaries of the solution-treated material are relatively free of carbide precipitation, whereas both the sensitized and stabilized samples exhibit heavy carbide precipitation in the boundaries, as shown in Figure 3. The carbide particles in the stabilized sample are somewhat coarser; however, the carbides in both cases are <3 microns in diameter, much smaller than the inclusions in stringers.

Scanning Electron Microscopy

Each group of samples were examined in the scanning electron microscope (SEM) and Table III summarizes observations made on samples prior to flashing with xenon light. The different heat treatments had a major influence on the surface condition of the steel after electropolishing. Chemical polishing alone did not produce any gross surface structure difference between the three heat treatments.

In the case of the solution-treated sample, where most of the grain boundary carbides are dissolved, electropolishing produced a very shiny, smooth surface finish. However, in both the stabilized and sensitized conditions, electropolishing produced a very irregular surface finish with preferential attack at the grain boundaries. The surface in both cases was pitted, quite different from the shiny surface of the solution-treated/electropolished samples shown in Figure 4. Carbide particles within the boundaries are more cathodic than the surrounding matrix, and thus, become exposed as the electropolishing process continues. Figure 5 compares the surface condition of samples given different heat treatments, electropolished, but not flashed.

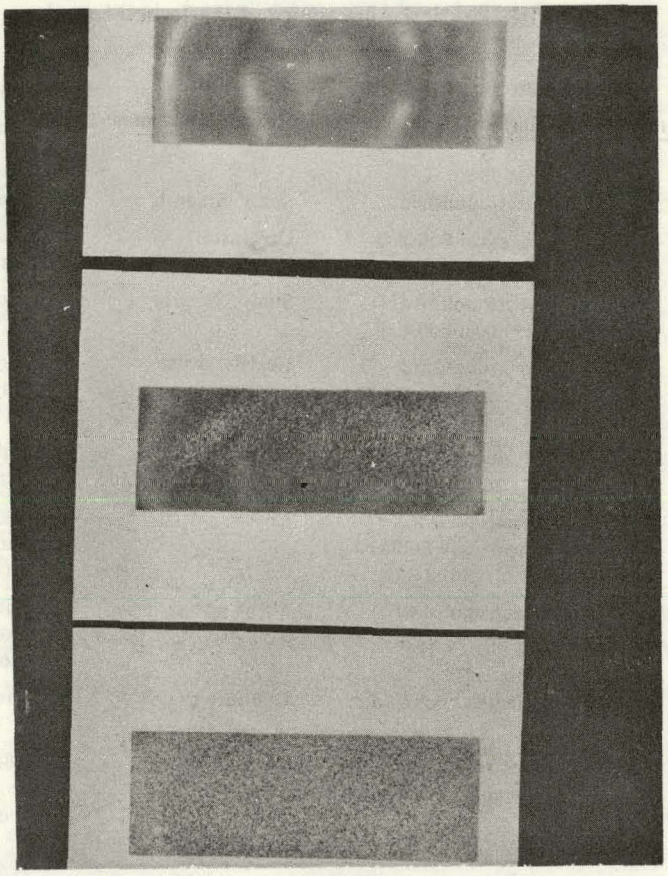

FIGURE 4. Surface Appearance of (a) Solution Treated, (b) Sensitized, and (c) Stabilized Samples after Electropolishing. Magnification 1.3X. Rings on (a) Due to Reflection of Camera Lense on Shiny Surface, White Speckled Pattern on (b) and (c) Due to Surface-Pitting.

Analysis of Damage Sites

Samples from each condition were flashed and the reactivity of xenon light with the metal surface was rated in terms of the number of damage sites observed on the glass capsule after flashing. Table IV summarizes these observations. Samples that were only heat treated and not subsequently polished showed a strong correlation between heat treatment and number of damage sites. The solution-treated and stabilized samples generated very few damage sites compared to the sensitized and as-received samples. This would be expected if the grain boundary mechanism postulated earlier were true, and it suggests that the different microstructures achieved by heat treatment have a major influence on the generation of damage sites. However, tests with specimens that were both heat treated and polished did not show any good correlations. It is not clear at this time whether polishing tends to negate any influence of heat treatment, or whether problems exist either in the testing procedure or

FIGURE 5. Comparison of Surface Condition of (a) Solution-Treated, (b) Stabilized, and (c) Sensitized Samples after Electropolishing. Magnification 500X.

(a)

(b)

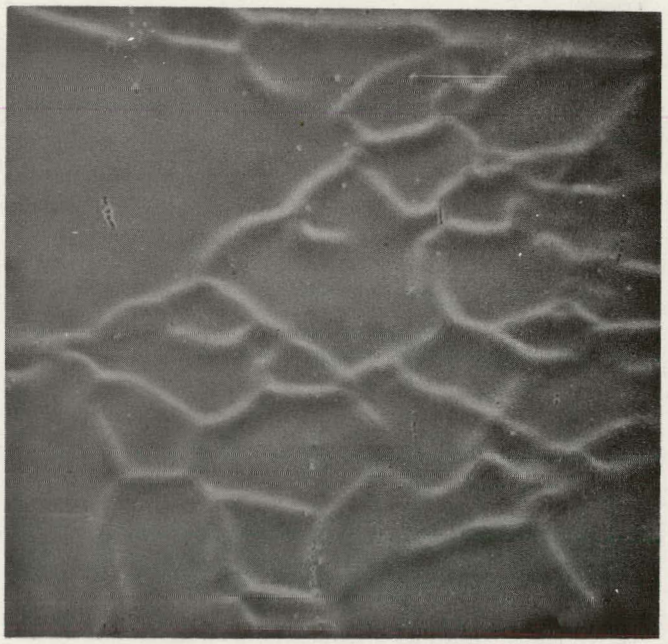

(c)

TABLE IV. Observed Damage Sites in Flashed Samples

Heat Treatment	Surface Treatment	Sample Number	Number of Metallic Damage Sites
As-received	–	1	30
Solution treated	–	2	2
	[a]EP	VK-11	1
	EP	VK-13	13
	EP	VH- 3	3
	[b]CP	VK- 9	2
	CP	VK-10	8
	CP	VH- 7	4
	EP + CP	VK- 7	6
	EP + CP	VK- 8	2
	EP + CP	VII- 2	0
Stabilized	–	3	3
	EP	VK-13	10
	EP	VK-14	6
	EP	VH -10	2
	CP	VK-19	5
	CP	VK-20	1
	CP	VH- 6	5
	EP + CP	VK-15	1
	EP + CP	VK-16	0
	EP + CP	VH- 5	0
Sensitized	–	4	15
	EP	VK- 5	2
	EP	VK- 6	12
	EP	VH- 8	0
	CP	VK- 3	1
	CP	VK- 4	16
	CP	VH- 9	2
	EP + CP	VK- 1	0
	EP + CP	VK- 2	1
	EP + CP	VII- 4	1

[a]EP Electropolish
[b]CP Chemical Polish

that the small carbide particles are not always visible on the capsule after flashing.

If there is a trend in the data, it is that the combined electropolishing and chemical polishing treatments for any of the heat treatments produced the minimum damage sites. The glass capsule is examined at low magnification and damage sites resulting from particles as small as 3 microns in diameter may be difficult to detect. Further tests are needed to determine if a correlation exists between heat treatment and number of damage sites.

Several damage sites were analyzed by energy dispersive x-rays, using the SEM, and a summary of these results are presented in Table V. In almost all cases, iron (Fe) was associated with the damage site. In addition to identifying pure Fe and pure nickel (Ni), [Fe, chromium (Cr)], [Fe, copper (Cu)], [Fe, titanium (Ti)], and (Fe, Ni) were associated within a damage site, with trace amounts of zinc (Zn), potassium (K), chlorine (Cl), and manganese (Mn) in some cases. The stainless steel pattern of Fe, Cr, Ni was found in two cases. Since the energy dispersive system is unable to detect

TABLE V. Analysis of Damage Sites

Sample	Damage Sites (Approximate Diameter of Site Microns)	Chemistry of Site
VH-2	250	Ni
VH-3	150	Fe
VH-6	500	Fe, Cu, Zn
VH-7	150	Fe, Cr
VH-7	50	Fe, Cr
VH-5	---	Fe, Cr, Ni
VK-4	50	Fe, Cr
VK-3	125	Fe, Cr
VK-6	800	Fe
VK-6	150	Fe, Ti
VK-6	100	Fe, Cu
		Fe, Cr, Ni
		Fe, K, Cl
VK-6	750	Fe, Ni
		Fe, Ti, Mn

FIGURE 6. Damage Site Containing Only Iron. Sample VH-3. Magnification 525X.

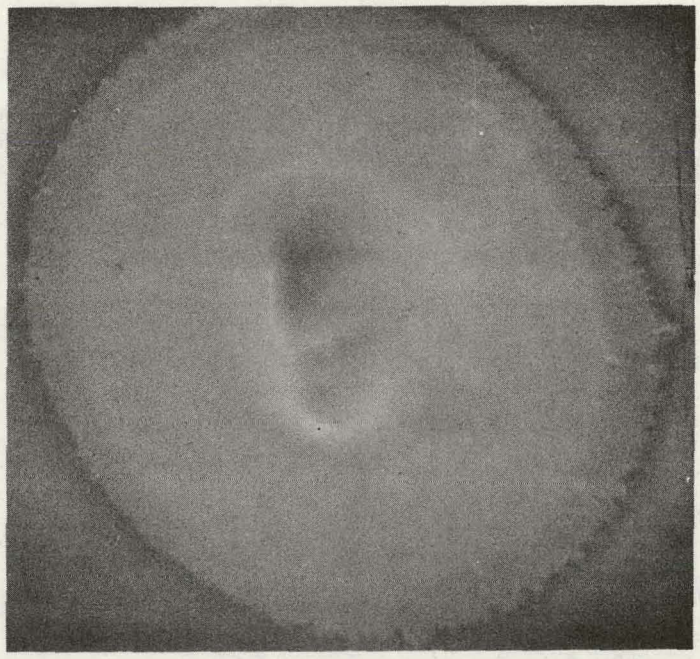

elements lighter than fluorine, it is not possible to determine if these metallic atoms are in the form of oxides, nitrides, or carbides. However, there is a strong possibility that some of the damage sites could result from $(Cr, Fe)_{23}C_6$ carbides, which are known to precipitate in grain boundaries as a result of sensitization or stabilization heat treatments.

The size of the damage sites are also consistent with the inclusion size observed in the as-received stock. Several different types of damage sites were observed. Figures 6 and 7 are sites which were found to contain only Fe. Figure 8 shows one that contained only Ni. Several sites contained Fe and Cr, as shown in Figures 9 and 10. The concentric rings in Figure 11 were

FIGURE 7. Damage Site Containing Only Iron. Sample VK-6. Magnification 85X.

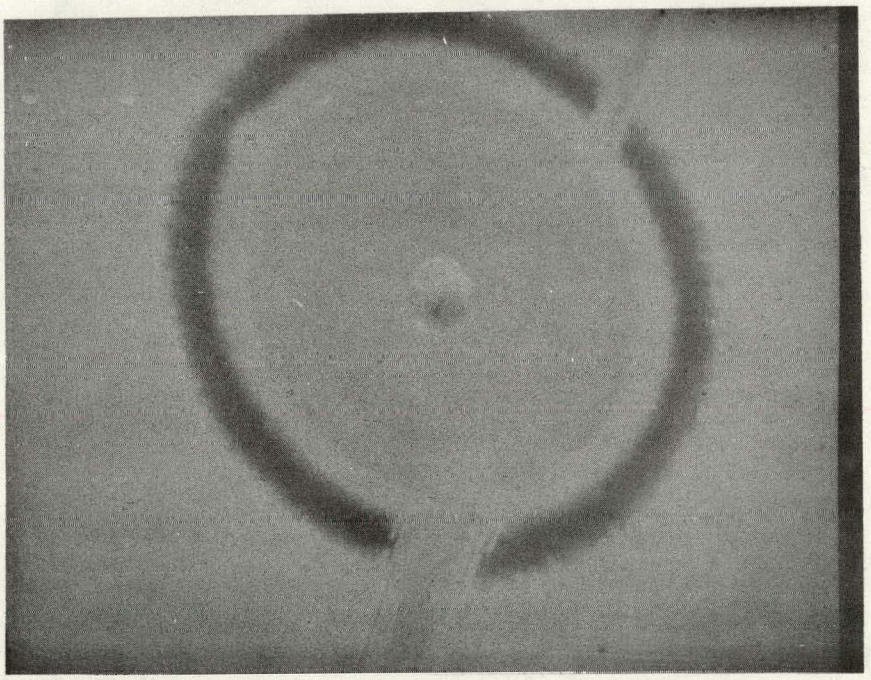

FIGURE 8. Damage Site Containing Only Nickel. Sample VH-2. Magnification 300X.

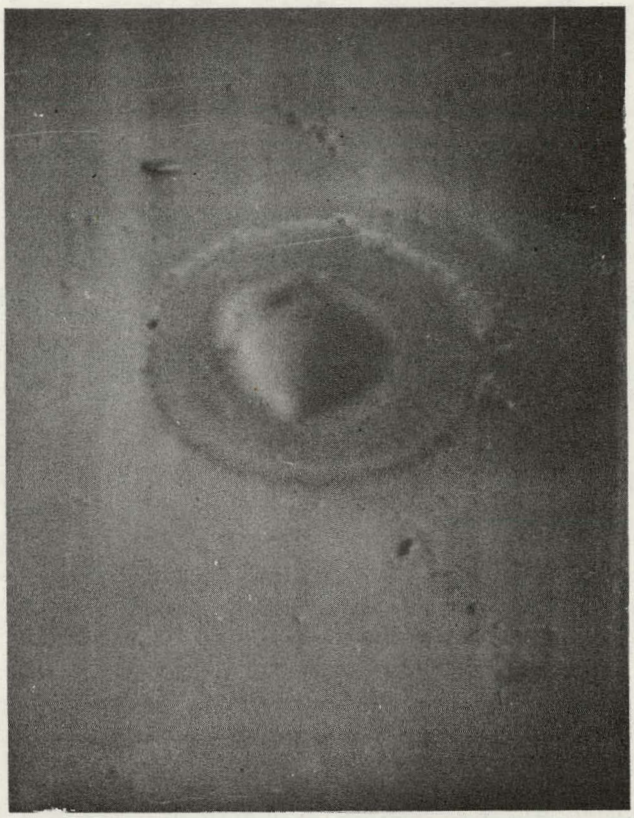

FIGURE 9. Damage Site Containing Iron and Chromium. Sample VH-7. Magnification 750X.

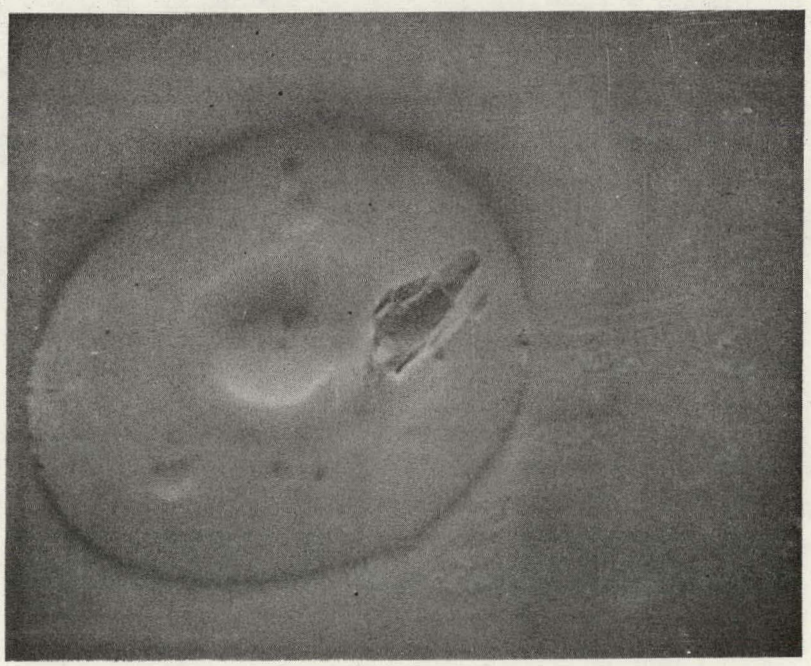

FIGURE 10. Damage Site Containing Iron and Chromium. Sample VH-7. Magnification 400X.

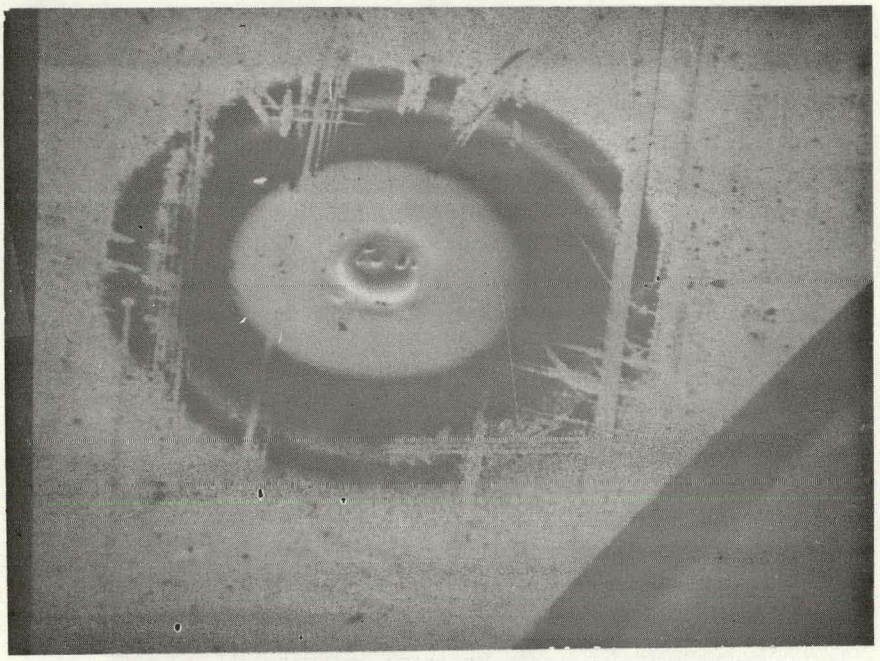

(a)

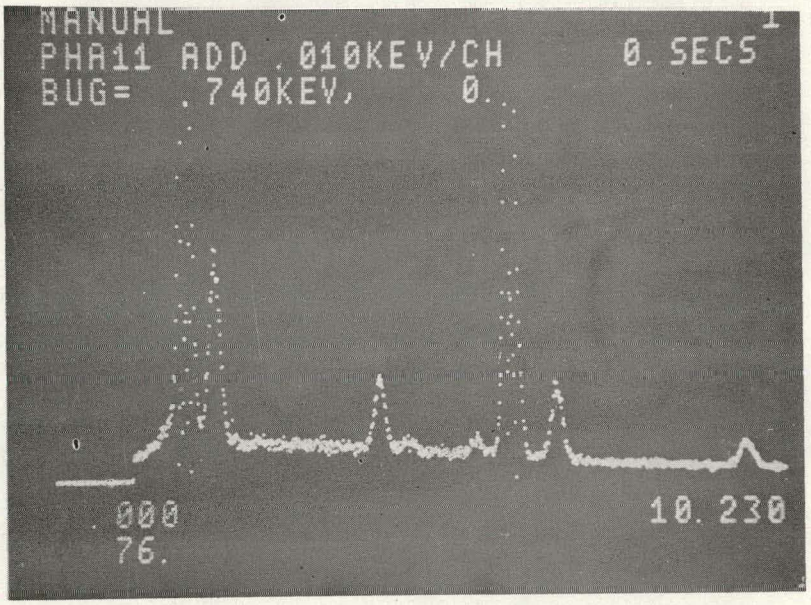

(b)

FIGURE 11. Damage Site (a) Containing Iron, Titanium, Manganese in Center, Iron + Nickel in Light Gray Region Around Center, Iron with Trace of Nickel in Black Ring. X-ray Spectrum (b) of Center, Silicon and Gold Due to Quartz Capsule and Sample Coating. Sample, VK-6. Magnification 85X.

found to contain (Fe, Ni) and (Fe, Ti, Mn). Manganese is an alloying element in the steel and its presence is not surprising. Titanium is used as a deoxidant in steelmaking, and its presence in the form of an oxide is possible. The association of Cu and Zn with Fe, shown in Figure 12, is more unusual.

FIGURE 12. Damage Site Containing Iron, Copper, and Zinc. Sample VH-6. Magnification 190X.

A variety of particles was found in the damage site shown in Figure 13 together with the respective x-ray spectrum. The large, white particle contains (Fe, K, Cl). The other two darker particles are stainless steel, which appear to be machine chips or burrs that were removed from the metal. The black spots are primarily Cu, and the major area of the damage site is Fe.

These results show that several chemical compounds are associated with damage sites. Although particles with a stainless steel composition were found, indicating that a chip of steel could have been removed from the surface, the majority of the sites analyzed contained Fe or (Fe, Cr) with minor amounts of Ni, Ti, Cu, and Mn in some cases. The chemistry and size of several of these sites indicate that inclusions and/or carbide are likely sources of contamination. This would be consistent with the hypothesis adopted in this work. It is not inconceivable that a 50 to 100 micron damage site could have been caused by a 3 micron particle.

DISCUSSION

The general surface appearance of samples before and after flashing with xenon light was compared using the SEM. No attempt was made in this initial study to compare a specific defect or region of a sample before and after flashing. General scans of the samples were made, taking typical photomicrographs in selected areas of the samples to determine if any gross structural changes occurred as a result of flashing.

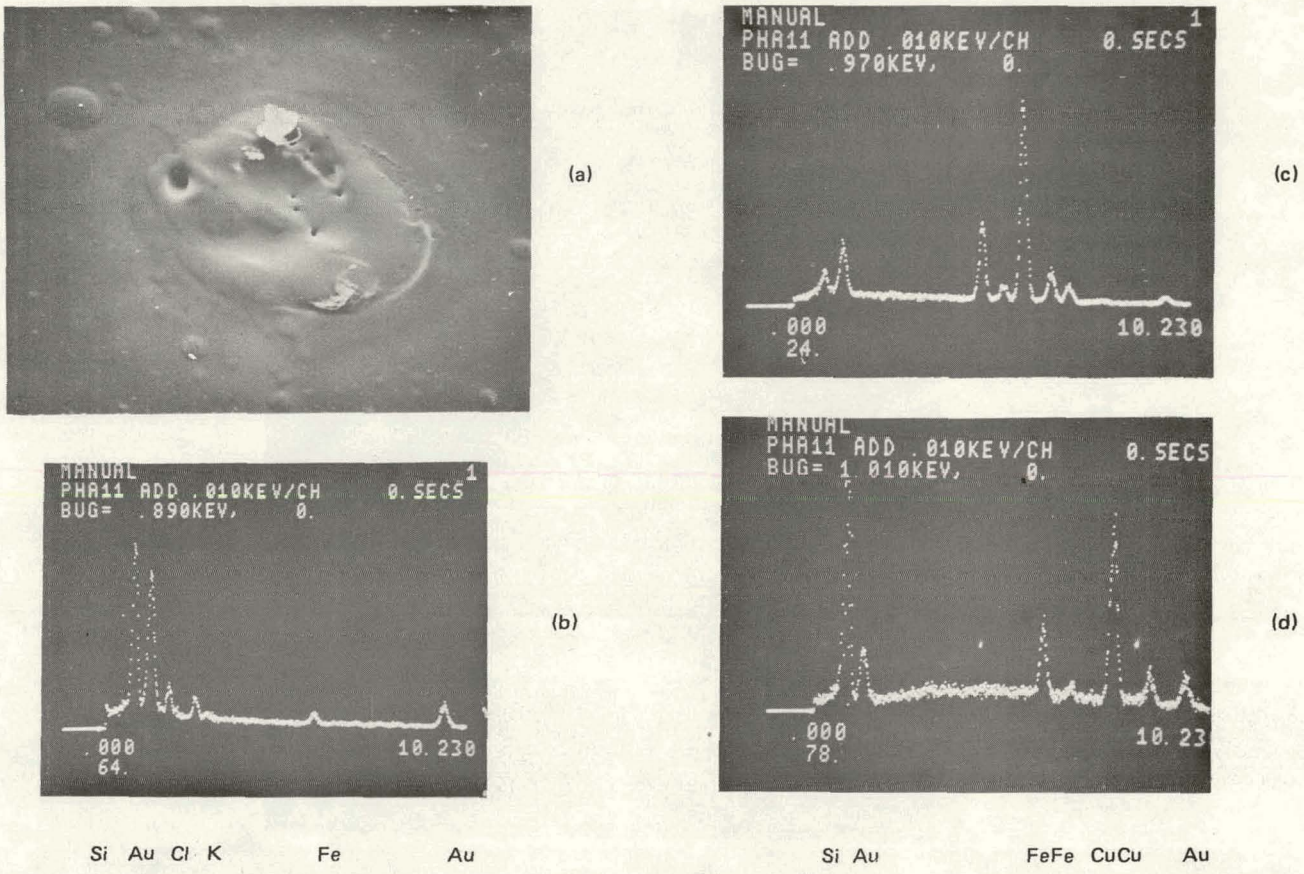

FIGURE 13. Multiple-Phase Damage Site (a) Containing Large White Particle Iron, Potassium, Chlorine, Two Smaller Particles Iron, Chromium, Nickel, and Black Spots Copper, (b) X-ray Spectrum of Large White Particle. Silicon and Gold Peaks are Due to Quartz Capsule and Gold Coating on Sample. Sample VK-6. Magnification 300X. (c) X-ray Spectrum of Iron, Chromium, Nickel, Stainless Steel Pattern, and (d) X-ray Spectrum of Copper and Iron Background. Sample VK-6. Magnification 300X.

Two general features were observed which showed a change in surface condition as a result of flashing. First, the appearance of coarse inclusions resulting from the stabilization treatment changed, as shown in Figure 14. The inclusions, both in the matrix and grain boundaries, in the preflashed sample are rounded and well-defined at the bottom of each pit, whereas in the flashed sample, the region around each inclusion appears to be flattened, indicating that some type of reaction has occurred. This could be due to localized melting within the inclusion region.

The other observed feature is interesting. In all cases, regardless of heat treatment or surface treatment, surface striations were observed after the samples were flashed. Figures 15, 16, and 17 illustrate this phenomenon. The striations are well-defined within each grain and follow definite crystallographic orientations. As shown in Figure 18, the striations change direction at a grain boundary, showing the mismatch in crystallographic orientation between adjacent grains. Change-in-direction is also apparent at twin boundaries, as shown in Figure 19.

When a metal is heated to a high temperature in certain environments, a reaction can occur between a gas and a metal which will cause a change in the surface configuration of the metal. This phenomenon, known as thermal etching, has been observed in many metals and alloys, and several excellent articles have been written on the

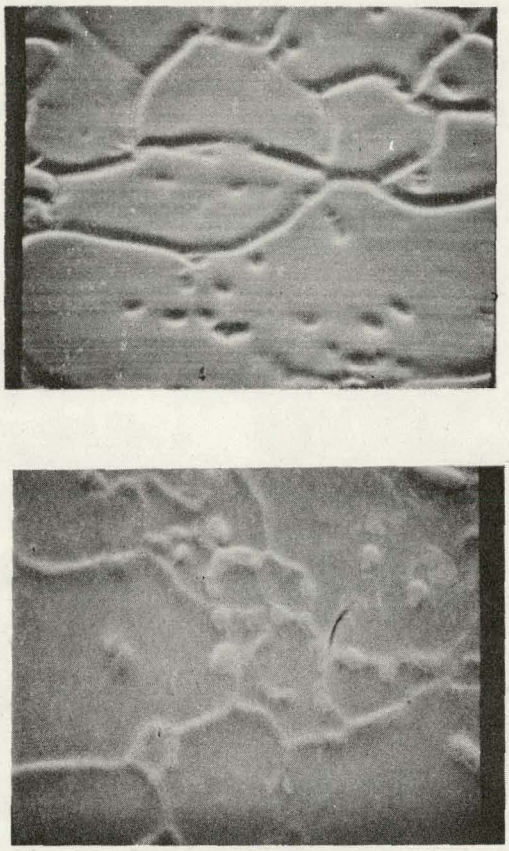

(a)

(b)

FIGURE 14. Comparison of Matrix and Grain Boundary Inclusions in a Stabilized, Electropolished and Chemical Polished Sample (a) Before, and (b) After Flashing. Sample VH-5. Magnification 300X.

subject (13, 14, 15, 16). Specific forms of thermal etching include thermal faceting, which produces striations consisting of parallel ridges formed from both low- and high-index planes within the matrix, and thermal grooving, where grain boundaries are enlarged by surface diffusion and/or evaporation. For any given set of conditions of temperature and gas pressure, thermal etching may occur to achieve a stable surface configuration by minimizing the surface-free energy of the metal. Processes such as surface diffusion, volume diffusion and evaporation are associated with thermal etching. Changes in the environmental conditions in contact with the metal surface can accelerate, inhibit, or actually reverse metal attack by thermal etching.

The discovery of striations, similar to that observed resulting from thermal etching, on the surface of flashed samples provides an important clue as to the fundamental mechanism causing damage in the laser amplifiers. All of the factors, i.e. presence of a partial pressure of nitrogen that can react with the Type 304 stainless steel surface, and a source of thermal energy in the form of high energy pulses of xenon light, are present to promote thermal etching. This phenomenon has been observed in many metals and alloys, and damage sites from unknown particles have also been observed in flash tests with several other metals. Pure metals such as Cu, Ag, Cr, Fe, Ni, Al, platinum (Pt), and Ti are all known to be susceptible to thermal faceting under certain conditions. This suggests that finding

FIGURE 15. Surface Striations on Flashed Sample. Sample VH-10. Magnification 500X.

FIGURE 16. Surface Striations and Grain Boundary Precipitates. Sample VH-10. Magnification 2000X.

FIGURE 17. Different Orientations of Striations Within Each Grain. Sample VK-1. Polarized Light. Magnification 400X.

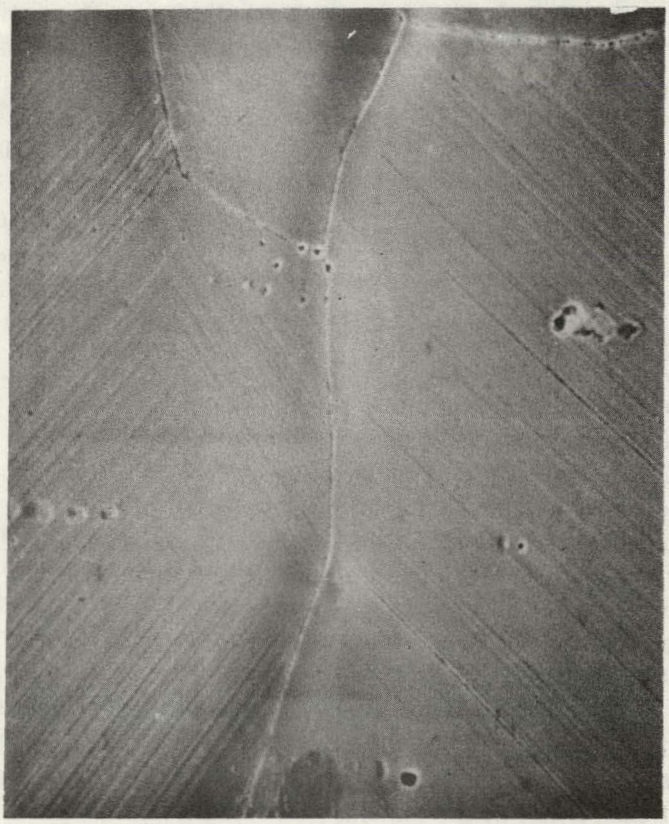

FIGURE 18. Orientation Mismatch of Striations at a Grain Boundary. Sample VH-4. Magnification 2000X.

FIGURE 19. Change in Crystallographic Orientation of Striations at a Twin Boundary. Sample VH-2. Polarized Light. Magnification 400X.

ways to make the metal surface immune to attack by thermal etching may eliminate the source of damage sites. Electropolishing and/or chemical polishing does not passivate the surface towards attack by thermal etching; however, preflashing may be effective in developing a stable surface configuration prior to use in the amplifier. The type and partial pressure of gas used in the amplifier is an important variable, and it is known that a change in the gas environment will affect the extent of thermal etching.

In addition, the combined effect of thermal etching on inclusions or carbides near the surface of the metal is unknown. Particles, either in the matrix or in grain boundaries, are potential sources of damage sites and can be dislodged due to surface roughening resulting from thermal etching. Localized heating around inclusions can be playing an important role. Various sources, such as preferential evaporation of metallic elements, volatilization of reaction products between nitrogen and the metal surface or volatilization of inclusions inherent in the metal are all potential sources. Analysis of damage sites show that different chemical compounds are involved, indicating that several sources are likely. Damage sites are certainly more complex than simply possessing a stainless steel composition.

Prior heat treatment history of the steel used to produce amplifier frames is important. Steel that has been fully solution treated produces the smoothest surface finish. Preferential attack of grain-boundary carbides during electropolishing produces a rougher surface on material that has been stabilized or sensitized. Carbides within the boundaries are more loosely bound to the metal and can be removed by the high energy xenon light. Also, evaporation losses within the grains, due to thermal etching, can expose other nonmetallic inclusions. This increases the potential for additional damage sites. Both factors can be contributing to the problem. Results from this study indicate that both a stable boundary and a stable surface configuration within the matrix may be required to eliminate particle contamination. Some combined solution treatment and preflashing treatment may be necessary. The microcleanliness of the steel is also important. Further work is needed to separate the various factors involved.

CONCLUSIONS

1. Analysis of damage sites shows that particles of different chemical compositions cause glass damage. Inclusions and/or carbides in the steel have to be a contributing factor.

2. The size of inclusions and carbides in the steel is consistent with the size of damage sites observed on the glass. It is possible that a thermally excited particle can produce a damage site approximately 2 to 10 times as large as its original size.

3. Electropolishing fully solution-treated Type 304 stainless steel produces the best surface finish. Carbide precipitation causes surface irregularities due to preferrential attack at the grain boundaries.

4. The size of carbides produced by the stabilized and sensitized treatments may be too small to detect a difference in quantity of damage sites resulting from the different heat treatments. This could explain the lack of correlation in the data. Extended heat treatment times to produce larger particles may be necessary to demonstrate effects of carbides.

5. High energy pulses of xenon light in a nitrogen environment thermally etches the steel surface. For all heat treatments and surface treatments studies, the surface is unstable to this type of thermal energy.

6. Preflashing to achieve a stable surface configuration may be effective in controlling damage sites.

7. Reducing inclusion content of the steel should reduce the probability of damage sites.

REFERENCES

1. K. T. Aust. "Intergranular Corrosion of Austenitic Stainless Steels." *Transactions TMS-AIME, Volume 245.* 2117 (1969).

2. R. J. Hodges. "Intergranular Corrosion in High Purity Ferritic Stainless Steels: Effect of Cooling Rate and Alloy Composition." *Corrosion, Volume 27.* 119 (1971).

3. S. Alm and R. Kiessling. "Chromium Depletion Around Grain-Boundary Precipitates in Austenitic Stainless Steel." *J. Inst. Metals. Volume 91.* 190 (1962).

4. K. T. Aust, J. S. Armijo, and J. H. Westbrook. "Heat Treatment and Corrosion Resistance of Austenitic Type 304 Stainless Steel." *Transactions ASM, Volume 59.* 544 (1966).

5. J. S. Armijo. "Intergranular Corrosion of Nonsensitized Austenitic Stainless Steel." *Corrosion, Volume 24.* 24 (1968).

6. M. A. Streicher. "General and Intergranular Corrosion of Austenitic Stainless Steels in Acids." *J. Electrochem. Soc., Volume 106.* 161 (1959).

7. A. B. Kinzel. "Chromium Carbide in Stainless Steel," *J. Metals, Volume 4.* 469 (1952).

8. H. H. Uhlig. *Corrosion and Corrosion Control.* John Wiley & Sons, New York. 2nd Edition 303. (1971).

9. N. Azzerri, L. Giuliani, and G. Bombara. "Influence of Surface Finish on Passivity Retention of Stainless Steels." *Corrosion, Volume 26.* 381 (1970).

10. A. Joshi and D. F. Stein. "Chemistry of Grain Boundaries and its Relation to Intergranular Corrosion of Austenitic Stainless Steel." *Corrosion, Volume 28.* 321 (1972).

11. R. Stickler and A. Vinckier. "Morphology of Grain-Boundary Carbides and its Influence on Intergranular Corrosion of 304 Stainless Steel." *Transactions ASM, Volume 54.* 362 (1961).

12. K. Ker. Lawrence Livermore Laboratory, Livermore, California. Private communication.

13. A. J. W. Moore. "Thermal Faceting," *Metal Surfaces, American Society for Metals.* Metals Park, Ohio. 155 (1963).

14. J. Moreau and J. Benard. "On Reversible Striations of Iron and its Alloys," *Acta Met., Volume 10.* 247 (1962).

15. E. D. Hondros and A. J. W. Moore. "Evaporation and Thermal Etching." *Acta Met., Volume 8.* 647 (1960).

16. A. J. W. Moore. "The Influence of Surface Energy on Thermal Etching." *Acta Met., Volume 6.* 293 (1958).